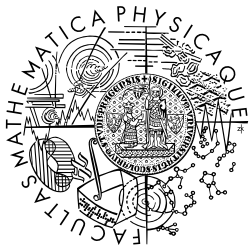

FACULTY
OF MATHEMATICS
AND PHYSICS
Charles University

Abstract of the doctoral thesis

Evolution of space weathering and its components – Effect of solar wind and microimpacts on reflectance spectra of airless planetary surfaces

Kateřina Flanderová

Astronomical Institute of Charles University

Supervisors of the doctoral thesis:	doc. Mgr. Josef Ďurech, Ph.D. doc. RNDr. Tomáš Kohout, Ph.D.
Study programme:	Theoretical Physics, Astronomy and Astrophysics
Study branch:	P4F1

Prague 2022

This doctoral thesis is the result of a double doctorate program and was done at the Astronomical Institute of Charles University and at the Department of Geosciences and Geography of the University of Helsinki between 2016 and 2022.

Ph.D. student: Mgr. Kateřina Flanderová

Departments: Astronomical Institute of Charles University
V Holešovičkách 2
180 00 Praha 8
Czech Republic

Department of Geosciences and Geography
PO Box 64 (Gustaf Hällströmin katu 2)
000 14 University of Helsinki
Finland

Supervisors: doc. Mgr. Josef Ďurech, Ph.D.
Astronomical Institute of Charles University
V Holešovičkách 2
180 00 Praha 8
Czech Republic

doc. RNDr. Tomáš Kohout, Ph.D. & Prof. Ilmo Kukkonen, Ph.D.
Department of Geosciences and Geography
PO Box 64 (Gustaf Hällströmin katu 2)
000 14 University of Helsinki
Finland

Pre-examiners: Prof. Ian Garrick-Bethell, Ph.D.
Earth & Planetary Sciences Department, University of California
1156 High Street
950 64 Santa Cruz, California
United States of America

Faith Vilas, Ph.D.
Planetary Science Institute
1700 East Fort Lowell
857 19 Tucson, Arizona
United States of America

Referee: Amanda Hendrix, Ph.D.
Planetary Science Institute
1700 East Fort Lowell
857 19 Tucson, Arizona
United States of America

The defence of the thesis will be held on November 4th 2022 at 1 p.m. in auditorium E204, Physicum, Kumpula campus, at the address Gustaf Hällströmin katu 2, Helsinki, Finland.

The thesis can be obtained in printed or electronic version through the Student Affairs Department of the Faculty of Mathematics and Physics of Charles University, Ke Karlovu 3, Praha 2.

Chairman of the programme P4F1: Prof. RNDr. Pavel Krtouš, Ph.D.
Institute of Theoretical Physics
V Holešovičkách 2
180 00 Praha 8
Czech Republic

Contents

Acknowledgements

During my doctoral studies, I was supported by the University of Helsinki Foundation and my work proceeded within institutional support RVO 67985831 supported by ESA Hera mission contracts at the Institute of Geology of the Czech Academy of Sciences. My travels were funded by Vilho, Yrjö and Kalle Foundation of the Finnish Academy of Science and Letters, and by DONASCI Travel grants. The thesis has made use of NASA Astrophysics Data System Bibliographic Services. I acknowledge the use of imagery from Lunar QuickMap (https://quickmap.lroc.asu.edu), a collaboration between NASA, Arizona State University & Applied Coherent Technology Corp.

Overview of research papers

This thesis is based on the following publications (in chronological order):

I **Chrbolková, K.***, Kohout, T., and Ďurech, J. (2019). Reflectance spectra of seven lunar swirls examined by statistical methods: A space weathering study. *Icarus*, 333, 516-527.

II **Chrbolková, K.***, Brunetto, R., Ďurech, J., Kohout, T., Mizohata, K., Malý, P., Dědič, V., Lantz, C., Penttilä, A., Trojánek, F., and Maturilli, A. (2021). Comparison of space weathering spectral changes induced by solar wind and micrometeoroid impacts using ion- and femtosecond-laser-irradiated olivine and pyroxene. *Astronomy & Astrophysics*, 654, A143.

III **Chrbolková, K.***, Halodová, P., Kohout, T., Ďurech, J., Mizohata, K., Malý, P., Dědič, V., Penttilä, A., Trojánek, F., and Jarugula, R. (2022). Sub-surface alteration and related change in reflectance spectra of space-weathered materials. *Astronomy & Astrophysics*, 665, A14.

*maiden name: **Chrbolková K.**, married name: **Flanderová, K.**

Authors' contribution to the publications

I	Study design:	T. K. and **K. F.**
	Material collection:	**K. F.**
	Analyses:	**K. F.**
	Interpretation:	**K. F.**, T. K., and J. Ď.
	Preparation of manuscript:	**K. F.**
	Corrections of manuscript:	J. Ď. and T. K.
II	Study design:	**K. F.**, T. K., R. B., and J. Ď.
	Measurements:	**K. F.**, R. B., K. M., P. M., V. D., C. L., F. T., and A. M.
	Analyses:	**K. F.**
	Interpretation:	**K. F.**, R. B., T. K., and J. Ď.
	Preparation of manuscript:	**K. F.**
	Corrections of manuscript:	R. B., T. K., and J. Ď.
III	Study design:	**K. F.**, T. K., and P. H.
	Material collection:	P. H.
	Analyses:	**K. F.**
	Interpretation:	**K. F.**, P. H., T. K., and A. P.
	Preparation of manuscript:	**K. F.**
	Corrections of manuscript:	J. Ď., P. H., and T. K.

Citations to the papers

This is a list of other authors' papers that cited the above-mentioned publications (list valid on 8th September 2022).

I Hess, M., et al. (2020). Processes governing the VIS/NIR spectral reflectance behavior of lunar swirls. *Astronomy & Astrophysics*, 639, A12.

Jordan, A. P. (2021). Evidence for dielectric breakdown weathering on the Moon. *Icarus*, 358, 114199.

Blewett, D. T., et al. (2021). Near-UV and near-IR reflectance studies of lunar swirls: Implications for nanosize iron content and the nature of anomalous space weathering. *Icarus*, 364, 114472.

Cho, E., et al. (2021). Reddening and darkening trends of on/off swirls and the relationship with magnetic field strength. *Publications of the Astronomical Society of Japan*, 73, 1604-1614.

II Lisse, C. M. and Steckloff, J. K. (2022). Thermal alteration and differential sublimation can create Phaethon's "rock comet" activity and blue color. *Icarus*, 381, 114995.

Preface

Asteroids (and other airless planetary bodies) are a very important group of bodies in the Solar system. Our knowledge of their mineralogy and physical conditions on the surface is nevertheless based mainly on remotely captured reflectance spectra. Interplanetary missions targeted at these bodies would give us more information but up to date there were only a few that reached them and supported us with detailed images and measurements, such as the Hayabusa mission (Abe et al., 2006; Hiroi et al., 2006). Spectroscopy is thus our best tool to learn about conditions on airless planetary bodies. To understand the spectroscopy of asteroids, one has to bear in mind that the spectra are influenced by many effects, such as temperature on the surface or roughness of the regolith layer. In this thesis, I focused on one of the major influences, i.e. space weathering.

The term space weathering refers to a set of processes, also called space weathering agents, which on timescales longer than 10^5 yr significantly alter the physical and chemical state of the topmost layers of the asteroid surfaces, see, for example, Clark et al. (2001); Pieters et al. (2000). As a result, the material on the silicate-rich airless planetary bodies darkens, the spectral slope increases, and the depths of the diagnostic absorption bands in visible (VIS) and near-infrared (NIR) reflectance spectra diminish.

In general, we know how to describe the spectral changes due to space weathering on airless planetary bodies. Nevertheless, we still lack knowledge on how individual space weathering agents influence the state of the surfaces and thus the reflectance spectra. In this thesis, I focused on finding the difference between the effect of the two most significant space weathering agents, i.e. solar wind irradiation and impacts of micrometeoroids, on reflectance spectra of airless planetary bodies.

I started by studying spectra from the areas of so-called lunar swirls, where we expect that the space weathering state is influenced mainly by micrometeoroid impacts. I have also, in cooperation with colleagues from France and Finland, conducted laboratory experiments during which we simulated the effect of individual space weathering agents and then evaluated changes in the reflectance spectra. And in the final stages of my Ph.D. studies, we examined our samples using electron microscopy to see the subsurface changes.

1 Introduction

In this section, I will briefly summarize the basics of the reflectance spectroscopy of minerals, the space weathering phenomenon, and the methods that were used for the completion of my dissertation. For a more extended version of the text, I refer the reader to the dissertation manuscript.

1.1 Theoretical background

1.1.1 Reflectance spectra of minerals

A reflectance spectrum is created in the following way: a photon reaches a boundary of two materials with different refractive indices. It either reflects from the boundary or refracts into the second material. Inside the material, the photon may get absorbed, by which it is lost and does not reach the surface again. Like this, the signal into the sensor is decreased and we see an absorption at the wavelength (energy) specific to the material.

In planetary spectroscopy, the main reason for absorptions are the transition metal ions immersed in the crystalline structure, mainly Fe^{2+}, but also other ions such as Mg^{2+}. Transition metal ions are characteristic by having their 3d orbital filled with six electrons. The presence of other ions in the crystalline structure causes distractions to the original energetic states in transition ions, which are then characteristic to the reflectance spectrum and cause (broad) absorption bands, which span across multiple wavelengths, not just the one relevant to the ion.

This dissertation focuses on two of the most common rock-forming minerals in the Solar system, i.e. olivine and pyroxene. The crystalline structure of both of them is based on silica-oxygen tetrahedrons. Between them, we may most frequently find the above-mentioned ions of Fe and Mg.

In olivine, $(Mg, Fe)_2SiO_4$, the metal ions occur in two different crystallographic sites, also known as M(1) and M(2). Visible and NIR spectra of olivine are characteristic by three overlapping absorptions at around 1 µm. The central absorption band origins in the M(2) site, while the two weaker absorptions at both sides of the central band are caused by M(1) site (Burns, 1970). For an example of olivine spectrum, see Fig. 1.

Spectra of pyroxenes, $(Ca, Mg, Fe)_2(Si, Al)_2O_6$, are characteristic by two major absorption bands at 1 µm and 2 µm, see Fig. 1. These two bands originate in the pyroxene M(2) site (Burns, 1989).

Changes to the spectral features

Several effects alter the reflectance spectra. For example, the bands shift to longer wavelengths with increasing amounts of Fe in the mineral. These shifts are more pronounced for olivines than for pyroxenes (Clark, 1999).

The temperature conditions on airless planetary bodies significantly influence the recorded spectrum. As the temperature increases, bands get wider, shift the positions of

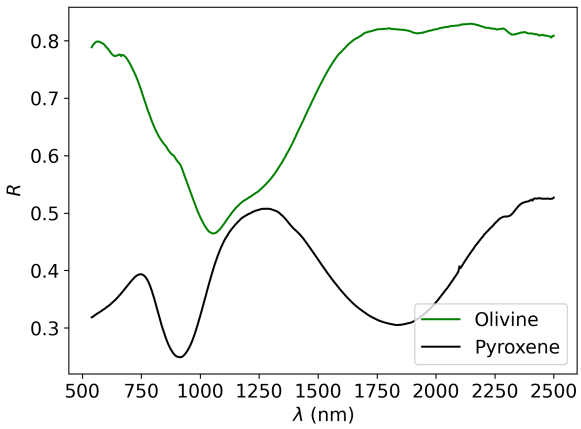

Figure 1: An example of a spectrum of olivine and pyroxene. Reflectance is denoted by R, wavelength by λ.

their minima, and as a consequence, even the band area ratios differ, see, for example, Burns (1989, Fig. 9).

Another factor influencing the spectral shape is the size of the regolith particles. The larger the particles in the sample are, the smaller the albedo is, the bluer the spectral slope is, and the deeper the absorption bands are (Reddy et al., 2015).

The phase angle is another factor influencing spectra. It is defined as an angle between the Sun, the body, and the probe or instrument measuring the spectrum. This viewing geometry influences the spectral slope, albedo, and the position and depth of the absorption bands. All these changes are due to the dependence of the reflectance curves on the observation geometry (Gradie et al., 1980).

1.1.2 Space weathering

Space weathering is another important factor influencing the physical and chemical properties of topmost hundreds of nm of airless planetary surfaces (Hapke, 2001; Pieters and Noble, 2016), and consequently their spectra. Space weathering does not refer to only one process but encompasses several processes the prime of which are the irradiation by solar wind ions and impacts of micrometeoroids (Hapke, 1965, 2001; Pieters et al., 2000; Pieters and Noble, 2016; Wehner et al., 1963).

In this thesis, I deal with silicate-rich bodies. It was found that as a result of space weathering, VIS-NIR spectra of these bodies darken (albedo decreases), darkening is more intense towards the shorter wavelengths (resulting in spectral slope reddening), and the characteristic mineral absorption bands fade away, see, for example, Hapke (2001). As a result, if we measure a spectrum of the space-weathered soil taken to the Earth by the Apollo missions, it does not match the spectrum of the preserved interior of the boulder crushed to the same particle size, see, for example, Hapke et al. (1970).

Cassidy and Hapke (1975) showed that space weathering, at least on the Moon, is caused by the creation of small particles of metallic iron, so-called nanophase iron particles ($npFe^0$). Nanophase iron may grow to larger sizes. Upon impacts, individual particles merge into larger structures, held together by impact glasses, also known as agglutinates (Keller et al., 1998; Noble et al., 2007). Both types of these particles are opaque and thus disable the repeated reflections in the material, which is the main reason for the darkening (Chapman, 2004). The main reasons for the creation of $npFe^0$ particles are melting caused by microimpacts and solar wind sputtering.

Lunar swirls and their space weathering

A lunar swirl is a curvilinear bright patch on the lunar surface, whose shape is not connected to the local topography. Lunar swirls may be found all over the lunar surface (Hood and Williams, 1989). When localized in lunar mare, the swirl is usually more complex in shape and the albedo contrast to the background material is stronger than in highlands, where the swirls tend to be simpler and less visible (Blewett et al., 2011). All lunar swirls are associated with increased magnetic field, so-called magnetic anomaly. A typical example of lunar swirl is the Reiner Gamma in Oceanus Procellarum or the Mare Ingenii swirl. Both show large spectral contrast and a complex shape. An example of the highland swirl is, e.g., the Gerasimovich anomaly, which is also the area of the strongest magnetic field on the Moon.

Soon after the discovery of lunar swirls, Schultz and Srnka (1980) suggested that the swirls originated in the cometary impact event. Other theories commented on meteorite impacts causing high enough temperatures for creation of magnetic fields. Nevertheless, this theory is inconsistent with the fact that Glotch et al. (2015) did not observe any changes of the cm-scale roughness or temperature of the swirl areas that would support such events in the Lunar Reconnaissance Orbiter Diviner Lunar Radiometer data. On the other hand, a newer study of Bhatt et al. (2021) comments on the differences in the regolith microstructure in the Reiner Gamma swirl compared to the surroundings. Some of the swirls are placed in antipodes to the big impact basins on the Moon (Hood and Williams, 1989). This led to a theory that the material ejected during the basin's creation circulated around the Moon and collided in the antipode, creating the swirl. Not all swirls are found in the antipodes though.

The main factor influencing the state of the lunar surface in the area of lunar swirl is the presence of the magnetic field. This field protects the surface from the majority of incoming charged particles (such as the solar wind ions). The ions are deflected and move along the magnetic field lines, by which they are concentrated into narrow areas of so-called dark lanes (Kramer et al., 2011). The theory of surface preservation from incoming ions is called the Magnetic field stand-off theory (Hood and Schubert, 1980; Hood and Williams, 1989).

The magnetic field stand-off does not influence the micrometeoroids, as they are not charged. The lunar swirls are believed to be $\approx 3.9\,\mathrm{Gyr}$ old (Blewett et al., 2011). Micrometeoroids would thus have a sufficiently long time to weather their surface. Another mechanism causing the bright nature of the swirls has thus been proposed. Neugebauer et al.

(1972) proposed that fine dust may be lifted by the terminator crossing and transported great distances. According to Stubbs et al. (2006), particles can be transported up to several kilometres on the surface of the Moon and bright highland material may get transported into the swirls.

Asteroidal space weathering

Generally, there are two types of asteroids: bright and dark ones. Based on the classification of DeMeo et al. (2009), the bright asteroids are those of Q-, S-, A-, R-, and V-type and these are the aim of my work. One of the prime motivations to study asteroidal space weathering is to understand the evolution of asteroidal families. The dynamical age of a family correlates with reddening of the spectra of its members, because we expect that the parent body of the family was fresh in its volume, and during the catastrophic collision, its inner parts became the surfaces of individual members of the family. The space weathering evolution state may thus be useful for identification of members of one family among other families, estimates of their evolution, etc.

Asteroidal space weathering studies originate in the disagreement between spectra of ordinary chondrite (OC) meteorites and their expected parent bodies, S-type asteroids (Brunetto et al., 2015). It was soon found out that if we apply changes consistent with space weathering to the OC spectra, we obtain remarkable similarity with S-type asteroidal spectra. It was also found that the Q-type asteroids are fresher analogues of S-type asteroids, see, for example, Binzel et al. (2004); Chapman (2004).

Based on findings of the Hayabusa mission to asteroid (25143) Itokawa, we know that similar to the lunar case the spectral changes may originate from the nanoparticles even at asteroids. In the case of Itokawa mainly of FeS and MgS, immersed in amorphous rims created by vapour deposition. Based on Brunetto et al. (2015), the observed particles do not contain agglutinates, as was seen on the Moon, which points to the lack of high-velocity impacts on the body. Also, based on the pictures of the surface, we can see that interplanetary dust particles may cause albedo variations at larger boulders. Generally, Itokawa shows considerable variations of brightness and colour corresponding to the presence of steep slopes and elevated areas (Hiroi et al., 2006). All of this is consistent with expectations about the space weathering behaviour.

Asteroid (4) Vesta shows only low levels of space weathering and its changes may, according to Pieters and Noble (2016), be associated mainly to the mixing with impactor material. The space weathering does not proceed in the lunar style there.

Typical space weathering timescales

The speed at which planetary surfaces weather is dependent on the environment they inhabit and also on their properties (Hapke, 2001; Pieters et al., 2000; Pieters and Noble, 2016). Firstly, the position of the body with reference to the Sun is important, as the flux of the solar wind particles changes with the square of the distance from the Sun. The conditions are thus different for the Near-Earth asteroids and for asteroids in the Main belt.

Also, the speed of micrometeoroids relative to the body is position-variable. It is expected that on Mercury, the amount of impact-induced melt is an order of magnitude larger than on the Moon (Bishop et al., 2019). Dependent on the position in the Solar system, other processes interconnected to space weathering become important, such as thermal cycling, which cracks the boulders, or sublimation on bodies rich in ices.

Additionally, there is a strong correlation with surface mineralogy, as the higher abundance of silicate minerals implies higher iron content and thus more material for creation of $npFe^0$ particles. Another factor is the surface texture, as it was shown that space weathering is dominant mainly in porous materials (Hapke, 2001), and spectral properties are influenced mainly by $< 45\,\mu m$ particles on the Moon.

Moreover, the time the surface is subject to the space environment is crucial for its weathering stage. Solar wind saturates the weathering state after $\approx 10^5\,yr$ at 1 au, but weathering by micrometeorites is $\approx$1000-times slower (Hapke, 1977; Noguchi et al., 2011; Yamada et al., 1999). Laboratory experiments showed that olivines are more easily weathered than pyroxenes (Yamada et al., 1999), which was later supported also by atomic-scale computational study of Quadery et al. (2015).

Even though asteroids are older than the typical weathering timescales, they do not generally look completely weathered. A group of processes rejuvenate their surfaces so they appear fresh. Small, non-catastrophic, impacts may overturn the topmost regolith layers of asteroids and uncover the fresh, underlying layers. Other rejuvenation processes are, for example, planetary encounters, spin-up by the YORP effect, or in the case of NEAs the thermal fatigue fragmentation (Brunetto et al., 2015).

1.1.3 Earlier laboratory experiments

Because of the sparsity of real space samples, laboratory irradiation experiments on terrestrial samples or meteorites are the most widespread mean of analyses aiming for a better understanding of the effects of space weathering. The two main space weathering agents are usually simulated by different types of experiments. Solar wind ions are represented by accelerated ions of light elements (see, for example, Lantz et al. (2017); Loeffler et al. (2009); Vernazza et al. (2013)), while micrometeoroid impacts are simulated mostly by laser irradiation (see, for example, Sasaki et al. (2002); Yamada et al. (1999); Fazio et al. (2018)).

Solar wind component

Ion irradiation experiments differ by the type of the ion used. Most of the studies up to date focused on the most common solar wind ions, i.e. hydrogen, H, and helium, He, that make up to 99 % of the total solar wind flux (see, for example, Brunetto and Strazzulla (2005); Brucato et al. (2004)). Some works also used heavier ions, to simulate other components of the solar wind (see, for example, Kaňuchová et al. (2010); Fulvio et al. (2012)).

Typically, the most common H^+ ion has an energy of about 1 keV, and He^+ ion has energy of approximately 4 keV. Nevertheless, many works used even more than 10 times greater energies, see, for example, Lantz et al. (2017). These studies thus simulated particles

from the solar flares, which are not as common as the regular, calm, solar wind but may also have a significant impact (Brunetto et al., 2015).

Micrometeoroid impacts component

The most widely used laser is yttrium-aluminium garnet doped by neodymium, with the typical wavelength of 1064 nm (see, for example, Corley et al., 2017; Sasaki et al., 2002). Usual pulse duration is between 6 ns and 8 ns, as this timescale is comparable to the duration of 1 µm–10 µm dust impacts (Yamada et al., 1999; Sasaki et al., 2002). Fazio et al. (2018) were the first who conducted a new type of experiments using femtosecond laser pulses. Based on their work, femtosecond pulses represent the reality of the micrometeoroid impact better as for high enough irradiance the created shock wave propagating through the sample resembles the actual impact, while nanosecond pulses just heat and melt the surface.

1.2 Methods of the work

My dissertation consists of three parts. In Paper I, I evaluated spectral changes on the surface of the Moon based on the downloaded spectra from the Chandrayaan-1 mission. Paper II describes the irradiation experiments, I did with the help of colleagues, and following observations of the spectral changes. Finally, in Paper III, I comment on the connection of the subsurface structural and chemical changes, obtained through electron microscopy, to the spectral alteration in my samples.

1.2.1 Modified Gaussian Model

Basically all parts of my thesis are based on a comparison of different spectra and also on a comparison of spectral parameters. To obtain the spectral parameters, a model of the spectrum needs to be introduced. In this thesis, I used the Modified Gaussian Model (MGM) by Sunshine et al. (1999). MGM estimates the basic spectral characteristics such as the spectral slope, depth of mineral absorption bands, their position, etc. (Sunshine et al., 1990). The spectrum is fitted in the space of natural logarithm of reflectance $\ln(R)$ and energy x. This combination allows for a simple mathematical summation of the spectral continuum C and absorption bands, based on the equation:

$$\ln R(x_k) = \sum_{i=1}^{l} m(x_k)_i + C = \sum_{i=1}^{l} m(x_k)_i + ax_k + b\,,$$

where a, b are the slope and intercept of the continuum, index $k = 1, \ldots, n$, n is the number of individual wavelengths of measured spectra, and $i = 1, \ldots, l$, l being the number of modified Gaussian distributions/mineral absorption bands in the spectrum. The modified Gaussian distribution m has the following form:

$$m(x_k)_i = s_i \exp\left(\frac{-(x_k^{-1} - \mu_i^{-1})^2}{2\sigma_i^2}\right),$$

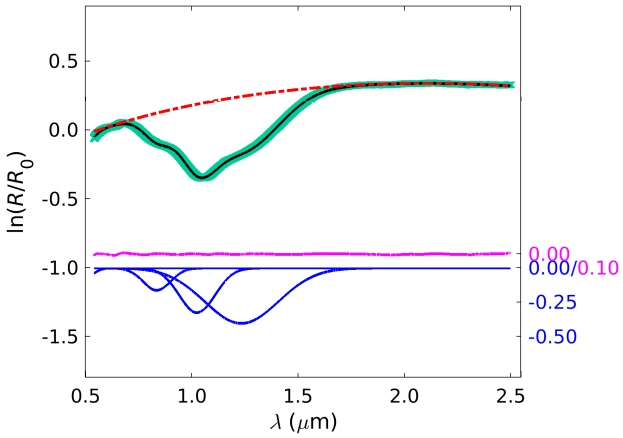

Figure 2: An example of fit of olivine spectrum using MGM. The green line represents the measured spectrum. The red dashed line is the continuum curve, the blue lines are individual modified Gaussian curves that summed together with the continuum result in the black line representing an overall fit. The purple line marks the error of the fit, R is the reflectance, R_0 reflectance of the fresh spectrum at 750 nm, and λ is the wavelength. Note that the y axis is in natural logarithm.

where s stands for the strength or amplitude of the distribution, μ is its centre (mean), and σ its standard deviation. The difference between the Gaussian (also called normal) and the modified Gaussian distributions is in the exponent $^{-1}$ in the $-(x_k^{-1} - \mu_i^{-1})^2$ parenthesis. An example of an olivine spectrum fitted using MGM is shown in Fig. 2.

1.2.2 Laboratory experiments

Irradiation of samples

A significant part of the dissertation is based on laboratory irradiation of pressed pellets of olivine and pyroxene powder. These pellets simulated asteroid surface as the powder on top was partially loose but the pellet as a whole was compact and easy to handle. The pellets were made of mineral material pressed onto the KBr base to ensure greater durability of the pellet without wasting the material. KBr is transparent to the spectroscopy in the wavelength range I used, and the layer of the mineral on top was optically thick enough to ensure that I studied only changes in the olivine/pyroxene.

The solar wind component was simulated by irradiation with three different types of ions. H^+ irradiation proceeded with the help of Kenichiro Mizohata, Ph.D. at the Accelerator laboratory of the University of Helsinki. We used 5-keV ions with fluence varying from 10^{14} ions/cm^2 to 10^{18} ions/cm^2. Different fluences simulated individual space weathering stages. The samples were surface passivated before extracting from the vacuum chamber, where the irradiation took place, to prevent from re-oxidation of potentially created npFe^0 particles.

He^+ and Ar^+ irradiation was done with the help of Cateline Lantz, Ph.D. and Rosario Brunetto, Ph.D. at L'Institut d'Astrophysique Spatiale (IAS-CSNSM), Orsay. The energies of the ions were higher than in the case of H^+, i.e. 20 keV and 40 keV. The great benefit of this experimental set-up was that we could measure the reflectance spectra in the same vacuum chamber where the irradiation took place and we could thus increase the irradiation stage in steps with using only one pellet.

To simulate micrometeoroid impacts, we built a new experimental set-up at the Department of Chemical Physics and Optics, Charles University together with Prof. Petr Malý, Ph.D. and František Trojánek, Ph.D. The set-up was inspired by work of Fazio et al. (2018). We shot individual 50-µm in diameter femtosecond laser pulses into a square grid on the pellet surface. The higher the density of the pulses was, the older surface we simulated. Similarly to the H^+ irradiation, we surface passivated the pellets before extracting them from the vacuum chamber and measuring their spectra.

Spectral measurements

After each irradiation, we conducted spectral measurements, either in situ or, after surface passivation in the shortest possible time, ex situ. The spectral measurements proceeded in three different laboratories based on the place where the irradiation took place. Each spectrometer had a slightly different wavelength range, but all of them showed spectra from 540 to 2500 nm. Even though the configuration of the spectrometers differed, I mainly compared relative trends in individual irradiation series, so there is no harm to the results.

H^+-irradiated samples were measured using the Gooch and Housego OL-750 automated spectroradiometric system at the Department of Physics, University of Helsinki. He^+- and Ar^+-irradiated samples were measured with Maya2000 Pro, OceanOptics, in VIS and Tensor 37, Bruker, in NIR at IAS. Lastly, the laser-irradiated pellets were measured using Vertex 80v, Bruker with A513/Q variable angle reflection accessory. This spectrometer allowed me also to measure all the samples even in the mid-infrared wavelength range.

Except for the spectra I measured (with the help of my colleagues), I used also other spectral curves, such as the lunar spectra from the Moon Mineralogy Mapper. These cover nearly the whole lunar surface (more than 95 %) in the wavelength range from 541 to 2976 nm, see e.g. Green et al. (2011) for more information. I also used asteroid spectra from DeMeo et al. (2009). From their dataset of 371 asteroids, I selected the bright ones. The spectra ranged from 400 to 2500 nm.

Electron microscopy

Samples irradiated by ions and laser were then subject to electron microscopy done mainly by Patricie Halodová, Ph.D. at the Science Centre Řež. The aim of the electron microscopy was to obtain information on the surficial and subsurface changes in the samples, their dependency on the space weathering agent/irradiation type, and their connection to the spectral changes.

Scanning electron microscopy aimed mainly at the changes in the surface structure and chemical conditions on the surface. I based the research mainly at images using the backscattered secondary electrons and on energy-dispersive X-ray analysis (EDS) of the elemental abundances. Transmission electron microscopy, on the other hand, aimed at the changes in the top-most 1 µm of the samples. My conclusions on subsurface alterations were then based mainly on bright-field transmission images and also on the EDS.

In addition to the above-mentioned, I have used several approaches, mainly from the field of statistical physics and also principal component analysis. Please see the full version of my dissertation for more details.

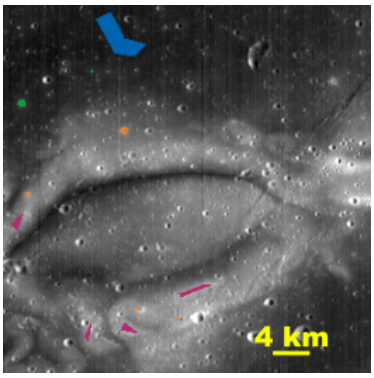

Figure 3: Reiner Gamma swirl with four different types of terrain I used for Paper I highlighted in different colours. The mature terrain influenced by all the space weathering agents is in blue, the fresh crater outside the swirl in green, the fresh crater inside the swirl in orange, and the swirl material influenced predominantly by micrometeoroid impacts is in magenta.

2 Overview of results

I will now briefly summarize what are the main results of the three papers, which are the core of this dissertation. The roman numbers match the assignment from page 2.

2.1 Paper I – Effect of micrometeoroids in lunar swirls

Paper I is based on an analysis of spectra from the areas of lunar swirls. Based on the solar wind stand-off theory, the surface of the Moon in the area of swirl is shielded by the magnetic field from the majority of incoming solar wind ions. As a result, the area is influenced mainly by micrometeoroid impacts. Using these areas, I thus could see what the spectra influenced by micrometeoroids look like and compare them to the spectra of the areas influenced by both the space weathering agents and to the areas of the pristine soil found in the impact craters, see Fig. 3 for an example of used areas.

Selecting seven different swirls from distinct locations around the Moon, I found two main dichotomies in the spectral evolution:

1. The mare/highland dichotomy in the albedo and 1 µm band depth behaviour. This dichotomy may potentially be prescribed to the different FeO content of the two types of terrain.

2. The near-/far-side dichotomy in the spectral slope behaviour, which probably results from the fact that the Moon is in the synchronous rotation with the Earth and the Earth's magnetotail is elongated with respect to the radial direction from the Sun. As a result, all the near-side swirls are subject to a decreased flux of solar wind ions compared to the far-side swirls.

Based on these two dichotomies, I posed constraints on the probability of the creation of lunar swirls by cometary impacts. I also indicated that the origin of the magnetic field in the area of lunar swirl is irrelevant to the rest of its evolution.

Based mainly on the observations of the principal component space, it was obvious that the micrometeoroid impacts do not induce the same complex of spectral changes as the solar wind ions.

2.2 Paper II – Irradiations of silicates

In Paper II, I describe the ion- and laser-irradiation experiments of olivine and pyroxene pellets. This set of experiments was designed to better understand the difference in the effect of the two space weathering agents on the spectra of the most common silicate-rich materials.

This paper shows three major results:

1. There is a difference between the effect of the ion and laser irradiation on the longer NIR wavelengths (at around 2 µm) that was prescribed to the different penetration depths of the laser and ions. In the VIS part of the spectra, this difference is not evident probably because of the dependence of the extinction coefficients of the darkening agents on the wavelength. We thus expect that this means that the solar wind irradiation can be distinguished from the micrometeoroid impacts at NIR wavelengths. See Fig. 4.

2. The above-mentioned difference was the only one I identified in the data. Otherwise, it seemed that the original mineralogy of the irradiated material had a greater significance for the spectral evolution than the space weathering agent. This was demonstrated on the time-evolution plots in which the change in any spectral parameter is similar for the given material and varying space weathering agent, but different for the two materials.

3. Based on the findings, I could make several conclusions on the evolution of individual observed asteroids in the Solar system, such as why (433) Eros shows albedo changes, but no significant variations of the spectral slope. This work also explained the high observed spectral slopes in the A-type asteroids.

2.3 Paper III – Subsurface changes and their connection to the spectra

The samples obtained during the irradiation experiments for Paper II were the source material for the next examination. In Paper III, I examined what the subsurface structure of the pellets was and how it correlates with the observed spectral changes. The scanning and transmission electron microscopy analyses were conducted by Patricie Halodová, Ph.D. at the Science Center Řež.

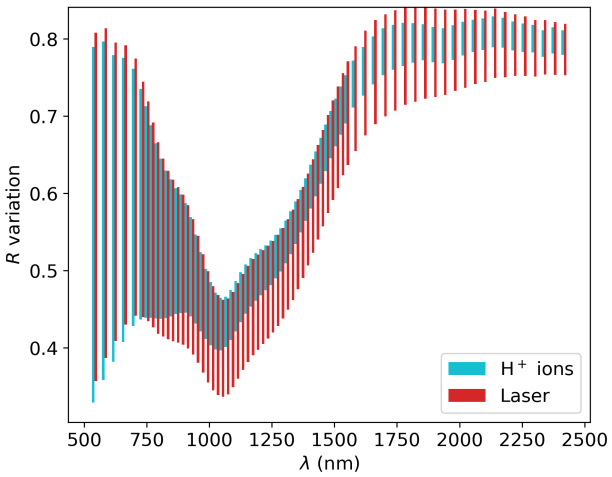

Figure 4: Spectral differences of laser and hydrogen ion (H^+) irradiation. Each bar connects at the upper end the reflectance, R, of the fresh material and at the lower end R of the irradiated material. The length of the bar thus shows the variation in R at the given wavelength, λ.

The main conclusion of this paper is that the main factor influencing the spectral changes is the presence of amorphous structures in the shallow subsurface layers that have sizes similar to the wavelength of incident light. I observed such structures in both H^+-irradiated samples and also in the laser-irradiated olivine. Laser-irradiated olivine additionally contained the nanophase iron particles (see Fig. 5) that also have a major impact on the spectra.

The only sample that did not contain such small structures was the pyroxene irradiated by laser. This sample also showed a very distinct evolution of the spectra, as it did not exhibit changes in the spectral slope, only changes in the depths of the absorption bands and constant darkening.

Based on these observations, I could construct the subsurface evolution scenario. In the beginning of the evolution, the material will suffer from the creation of small vesicles in partially amorphous layers induced by solar wind ions. The subsurface changes will cause rapid changes to the VIS slope. Later, the nanophase iron particles will appear which will contribute to the alteration of the NIR spectral slope as well. Only in the later stages will the spectral slope changes cease as the wavelength-sized structures will be overcome by the growing vesicles and thickened amorphous layer caused by an increased contribution of the micrometeoroid impacts.

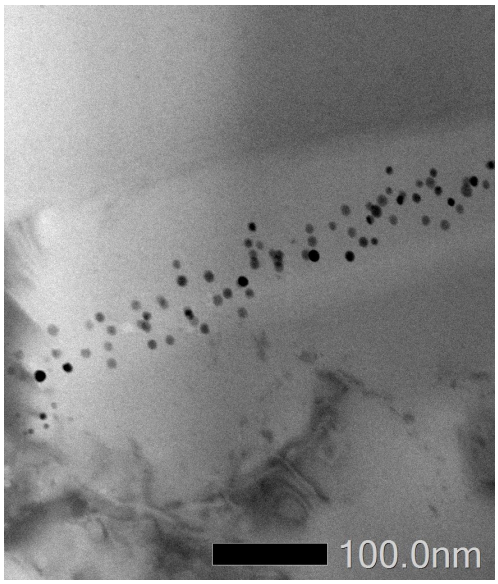

Figure 5: Transmission electron microscopy image of a focused ion beam section of olivine sample irradiated by laser. NpFe^0 particles are the dark dots in a layer. The top of the image represents a completely amorphous layer close to the pellet surface.

3 Conclusions

My thesis has the following main conclusions:

- Spectral changes due to space weathering are more dependent on the original mineralogy of surface than on the space weathering agent.
- Micrometeoroid impacts do not cause the same extent of changes as the solar wind irradiation or the two effects combined.
- The two space weathering agents are discernable based on evolution of spectra in the region around 2 µm. In this region, micrometeoroid bombardment causes greater changes than solar wind irradiation.
- The VIS spectral slope changes more significantly upon ion irradiation than micrometeoroid impacts.
- H^+ irradiation influences surface morphology differently to the micrometeoroid impacts.
- Spectral changes are dependent on dimensions and level of amorphisation of subsurface layers and on the presence of nanophase iron particles.
- Evolution of a silicate-rich spectrum will start in the VIS spectral slope changes. Later, also the NIR spectral slope will change in case nanophase iron particles develop in the material. Finally, the spectral slope will stop developing and only the absorption bands will evolve.

My conclusions are nevertheless based mostly on experiments done using two minerals. In future, it would thus be beneficial to proceed and do the experiments with some other minerals, such as plagioclase feldspar, as well. By these we could verify the conclusion on the dependence of space-weathering-related spectral changes on the mineralogy of the surface. Deeper understanding of the space weathering phenomenon may also be acquired through new or up to date least used methods, such as the electron microscopy. I am very much looking forward to the results of the upcoming interplanetary mission which will focus among other also on the space weathering phenomenon, such as the Hera mission to asteroid (65803) Didymos, or the Lunar Vertex mission to the Reiner Gamma anomaly.

Other relevant experience

The following tables summarize my participation in international conferences, for which I submitted abstracts/contributions listed below, and my foreign cooperation during the Ph.D. studies.

year	conference/meeting	location	contribution
2017	Week of Doctoral Students	Prague, CZE	talk (1)
2017	Workshop on Spectroscopy, photometry, and polarimetry of airless Solar system objects	Tuusula, FIN	talk (2)
2018	Lunar & Planetary Science Conference	Houston, TX, USA	poster (3)
2018	Workshop in Geology and Geophysics of the Solar System	Petnica, SRB	poster (4)
2019	Lunar & Planetary Science Conference	Houston, TX, USA	poster (5)
2021	Lunar & Planetary Science Conference	online	poster (6)
2021	Europlanet Science Congress	online	poster (7)
2021	Hayabusa symposium 2021	online	poster (8)
2022	Lunar & Planetary Science Conference	Houston, TX, USA	poster (9)

Table 1: Conferences and meetings summary.

(1) Chrbolková, K.*, Ďurech, J., and Kohout, T. (2017). Space Weathering on Airless Planetary Bodies. WDS'17 Proceedings of Contributed Papers – Physics, 41-45.

(2) Chrbolková, K.*, Ďurech, J., and Kohout, T. (2017). Use of lunar spectra for space weathering study.

(3) Chrbolková, K.*, Kohout, T., and Ďurech, J. (2018). Space Weathering Trends on the Moon Based on Statistical Analysis of Spectral Parameters. LPI Contribution No. 2083, id.1878.

(4) Chrbolková, K.*, Kohout, T., and Ďurech, J. (2018). Space Weathering Trends on the Moon.

(5) Chrbolková, K.*, Kohout, T., and Ďurech, J. (2019). Statistical Analysis of Lunar Swirls' Spectral Parameters Relevant to Space Weathering. LPI Contribution No. 2132, id.1034.

(6) Chrbolková, K.*, Brunetto, R., Ďurech, J., Kohout, T., Mizohata, K., Malý, P., Dědič, V., Lantz, C., Penttilä, A., Trojánek, F., and Maturilli, A. (2021). Comparison of Space Weathering Spectral Changes Induced by Solar Wind and Micrometeoroid Impacts. LPI Contribution No. 2548, id.1246.

(7) Chrbolková, K.*, Brunetto, R., Ďurech, J., Kohout, T., Mizohata, K., Malý, P., Dědič, V., Lantz, C., Penttilä, A., Trojánek, F., and Maturilli, A. (2021). Ion- and laser-weathered spectra: How (dis)similar are they? id. EPSC2021-565.

(8) Chrbolková, K.*, Brunetto, R., Ďurech, J., Kohout, T., Mizohata, K., Malý, P., Dědič, V., Lantz, C., Penttilä, A., Trojánek, F., and Maturilli, A. (2021). Comparison of ion- and laser-weathered spectra of olivines and pyroxenes.

(9) Chrbolková, K.*, Halodová, P., Kohout, T., Ďurech, J., Mizohata, K., Malý, P., Dědič, V., Penttilä, A., Trojánek, F., and Jarugula, R. (2022). Connection of Subsurface Structure of H^+- and Laser-Irradiated Samples to the Spectral Evolution. LPI Contribution No. 2678, 2022, id.1832.

*maiden name: Chrbolková K., married name: Flanderová, K.

year	other activities	place
2017	research visit	Lunar & Planetary Institute, Houston, TX, USA
2018	research visit	Lunar & Planetary Institute, Houston, TX, USA
2019	laboratory experiments	Institut d'Astrophysique Spatiale, Orsay, FRA
2020	laboratory experiments	SOLEIL, Saint-Aubin, FRA

Table 2: Other relevant international activities related to the Ph.D. studies.

Research visits were mainly aimed at discussions on my current work and understanding of the lunar spectra. Primary contact person was Georgiana Kramer, Ph.D. Laboratory experiments were conducted in cooperation with Rosario Brunetto, Ph.D., Cateline Lantz, Ph.D., and Stefano Rubino and their results may be seen, e.g. in my paper from 2021.

References

Abe, M., Takagi, Y., Kitazato, K., Abe, S., Hiroi, T., Vilas, F., Clark, B. E., Abell, P. A., Lederer, S. M., Jarvis, K. S., Nimura, T., Ueda, Y., and Fujiwara, A. (2006). Near-Infrared Spectral Results of Asteroid Itokawa from the Hayabusa Spacecraft. *Science*, 312(5778):1334–1338.

Bhatt, M., Wöhler, C., Aravind, K., Ganesh, S., and Bharadwaj, A. (2021). Regolith Characteristics of the Reiner Gamma Swirl as Revealed by Polarimetric Observations. In *52nd Lunar and Planetary Science Conference*, Lunar and Planetary Science Conference, page 2430.

Binzel, R. P., Rivkin, A. S., Stuart, J. S., Harris, A. W., Bus, S. J., and Burbine, T. H. (2004). Observed spectral properties of near-Earth objects: results for population distribution, source regions, and space weathering processes. *Icarus*, 170:259–294.

Bishop, J. L., Bell, III , J. F., and Moersch, J. E. (2019). *Remote Compositional Analysis: Techniques for Understanding Spectroscopy, Mineralogy, and Geochemistry of Planetary Surfaces.* Cambridge Planetary Science. Cambridge University Press.

Blewett, D. T., Coman, E. I., Hawke, B. R., Gillis-Davis, J. J., Purucker, M. E., and Hughes, C. G. (2011). Lunar swirls: Examining crustal magnetic anomalies and space weathering trends. *J. Geophys. Res. (Planets)*, 116.

Brucato, J. R., Strazzulla, G., Baratta, G., and Colangeli, L. (2004). Forsterite amorphisation by ion irradiation: Monitoring by infrared spectroscopy. *Astronomy and Astrophysics*, 413:395–401.

Brunetto, R., Loeffler, M. J., Nesvorný, D., Sasaki, S., and Strazzulla, G. (2015). *Asteroid Surface Alteration by Space Weathering Processes*, pages 597–616.

Brunetto, R. and Strazzulla, G. (2005). Elastic collisions in ion irradiation experiments: A mechanism for space weathering of silicates. *Icarus*, 179(1):265–273.

Burns, R. G. (1970). *Mineralogical Applications of Crystal Field Theory*, chapter Electronic spectra of transition metal ions in silicate minerals, page 83. Cambridge University Press.

Burns, R. G. (1989). Spectral mineralogy of terrestrial planets: Scanning their surfaces remotely. *Mineralogical Magazine*, 53.

Cassidy, W. and Hapke, B. (1975). Effects of darkening processes on surfaces of airless bodies. *Icarus*, 25:371–383.

Chapman, C. R. (2004). Space Weathering of Asteroid Surfaces. *Annual Review of Earth and Planetary Sciences*, 32:539–567.

Clark, B. E., Lucey, P., Helfenstein, P., Bell, J. F., I., Peterson, C., Veverka, J., McConnochie, T., Robinson, M. S., Bussey, B., Murchie, S. L., Izenberg, N. I., and Chapman, C. R. (2001). Space weathering on Eros: Constraints from albedo and spectral measurements of Psyche crater. *Meteoritics and Planetary Science*, 36(12):1617–1637.

Clark, R. N. (1999). *Spectroscopy of Rocks and Minerals, and Principles of Spectroscopy*, pages 3–52.

Corley, L. M., Gillis-Davis, J. J., and Schultz, P. H. (2017). A Comparison of Kinetic Impact and Laser Irradiation Space Weathering Experiments. In *Lunar and Planetary Science Conference*, volume 48 of *Lunar and Planetary Inst. Technical Report*, page 1721.

DeMeo, F. E., Binzel, R. P., Slivan, S. M., and Bus, S. J. (2009). An extension of the Bus asteroid taxonomy into the near-infrared. *Icarus*, 202:160–180.

Fazio, A., Harries, D., Matthäus, G., Mutschke, H., Nolte, S., and Langenhorst, F. (2018). Femtosecond laser irradiation of olivine single crystals: Experimental simulation of space weathering. *Icarus*, 299:240–252.

Fulvio, D., Brunetto, R., Vernazza, P., and Strazzulla, G. (2012). Space weathering of Vesta and V-type asteroids: new irradiation experiments on HED meteorites. *Astronomy and Astrophysics*, 537.

Glotch, T. D., Bandfield, J. L., Lucey, P. G., Hayne, P. O., Greenhagen, B. T., Arnold, J. A., Ghent, R. R., and Paige, D. A. (2015). Formation of lunar swirls by magnetic field standoff of the solar wind. *Nature Communications*, 6.

Gradie, J., Veverka, J., and Buratti, B. (1980). The effects of scattering geometry on the spectro-photometric properties of powdered material. *Lunar and Planetary Science Conference Proceedings*, 1:799–815.

Green, R. O., Pieters, C., Mouroulis, P., Eastwood, M., Boardman, J., Glavich, T., Isaacson, P., Annadurai, M., Besse, S., Barr, D., Buratti, B., Cate, D., Chatterjee, A., Clark, R., Cheek, L., Combe, J., Dhingra, D., Essandoh, V., Geier, S., Goswami, J. N., Green, R., Haemmerle, V., Head, J., Hovland, L., Hyman, S., Klima, R., Koch, T., Kramer, G., Kumar, A. S. K., Lee, K., Lundeen, S., Malaret, E., McCord, T., McLaughlin, S., Mustard, J., Nettles, J., Petro, N., Plourde, K., Racho, C., Rodriquez, J., Runyon, C., Sellar, G., Smith, C., Sobel, H., Staid, M., Sunshine, J., Taylor, L., Thaisen, K., Tompkins, S., Tseng, H., Vane, G., Varanasi, P., White, M., and Wilson, D. (2011). The Moon Mineralogy Mapper (M^3) imaging spectrometer for lunar science: Instrument description, calibration, on-orbit measurements, science data calibration and on-orbit validation. *J. Geophys. Res. (Planets)*, 116.

Hapke, B. (1965). Effects of a Simulated Solar Wind on the Photometric Properties of Rocks and Powders. *Annals of the New York Academy of Sciences*, 123:711–721.

Hapke, B. (1977). Interpretations of optical observations of Mercury and the moon. *Physics of the Earth and Planetary Interiors*, 15:264–274.

Hapke, B. (2001). Space weathering from Mercury to the asteroid belt. *J. Geophys. Res.*, 106:10039–10074.

Hapke, B. W., Cohen, A. J., Cassidy, W. A., and Wells, E. N. (1970). Solar radiation effects on the optical properties of Apollo 11 samples. *Geochimica et Cosmochimica Acta Supplement*, 1:2199.

Hiroi, T., Abe, M., Kitazato, K., Abe, S., Clark, B. E., Sasaki, S., Ishiguro, M., and Barnouin-Jha, O. S. (2006). Developing space weathering on the asteroid 25143 Itokawa. *Nature*, 443:56–58.

Hood, L. L. and Schubert, G. (1980). Lunar magnetic anomalies and surface optical properties. *Science*, 208:49–51.

Hood, L. L. and Williams, C. R. (1989). The lunar swirls - Distribution and possible origins. In Ryder, G. and Sharpton, V. L., editors, *Lunar and Planetary Science Conference Proceedings*, volume 19 of *Lunar and Planetary Science Conference Proceedings*, pages 99–113.

Kaňuchová, Z., Baratta, G. A., Garozzo, M., and Strazzulla, G. (2010). Space weathering of asteroidal surfaces. Influence on the UV-Vis spectra. *Astronomy and Astrophysics*, 517.

Keller, L. P., Wentworth, S. J., and McKay, D. S. (1998). Space Weathering: Reflectance Spectroscopy and TEM Analysis of Individual Lunar Soil Grains. In *Lunar and Planetary Science Conference*, volume 29 of *Lunar and Planetary Science Conference*.

Kramer, G. Y., Besse, S., Dhingra, D., Nettles, J., Klima, R., Garrick-Bethell, I., Clark, R. N., Combe, J.-P., Head, III, J. W., Taylor, L. A., Pieters, C. M., Boardman, J., and McCord, T. B. (2011). M^3 spectral analysis of lunar swirls and the link between optical maturation and surface hydroxyl formation at magnetic anomalies. *J. Geophys. Res. (Planets)*, 116.

Lantz, C., Brunetto, R., Barucci, M. A., Fornasier, S., Baklouti, D., Bourçois, J., and Godard, M. (2017). Ion irradiation of carbonaceous chondrites: A new view of space weathering on primitive asteroids. *Icarus*, 285:43–57.

Loeffler, M. J., Dukes, C. A., and Baragiola, R. A. (2009). Irradiation of olivine by 4 keV He^+: Simulation of space weathering by the solar wind. *Journal of Geophysical Research (Planets)*, 114(E3).

Neugebauer, M., Snyder, C. W., Clay, D. R., and Goldstein, B. E. (1972). Solar wind observations on the lunar surface with the Apollo-12 ALSEP. *Planetary and Space Science*, 20:1577–1591.

Noble, S. K., Pieters, C. M., and Keller, L. P. (2007). An experimental approach to understanding the optical effects of space weathering. *Icarus*, 192:629–642.

Noguchi, T., Nakamura, T., Kimura, M., Zolensky, M. E., Tanaka, M., Hashimoto, T., Konno, M., Nakato, A., Ogami, T., Fujimura, A., Abe, M., Yada, T., Mukai, T., Ueno, M., Okada, T., Shirai, K., Ishibashi, Y., and Okazaki, R. (2011). Incipient Space Weathering Observed on the Surface of Itokawa Dust Particles. *Science*, 333:1121.

Pieters, C. M. and Noble, S. K. (2016). Space weathering on airless bodies. *J. Geophys. Res. (Planets)*, 121:1865–1884.

Pieters, C. M., Taylor, L. A., Noble, S. K., Keller, L. P., Hapke, B., Morris, R. V., Allen, C. C., McKay, D. S., and Wentworth, S. (2000). Space weathering on airless bodies: Resolving a mystery with lunar samples. *Meteorit. Planet. Sci.*, 35:1101–1107.

Quadery, A. H., Pacheco, S., Au, A., Rizzacasa, N., Nichols, J., Le, T., Glasscock, C., and Schelling, P. K. (2015). Atomic-scale simulation of space weathering in olivine and orthopyroxene. *Journal of Geophysical Research (Planets)*, 120(4):643–661.

Reddy, V., Dunn, T. L., Thomas, C. A., Moskovitz, N. A., and Burbine, T. H. (2015). *Mineralogy and Surface Composition of Asteroids*, pages 43–63.

Sasaki, S., Hiroi, T., Nakamura, K., Hamabe, Y., Kurahashi, E., and Yamada, M. (2002). Simulation of space weathering by nanosecond pulse laser heating: dependence on mineral composition, weathering trend of asteroids and discovery of nanophase iron particles. *Advances in Space Research*, 29(5):783 – 788.

Schultz, P. H. and Srnka, L. J. (1980). Cometary collisions on the Moon and Mercury. *Nature*, 284:22–26.

Stubbs, T. J., Vondrak, R. R., and Farrell, W. M. (2006). A dynamic fountain model for lunar dust. *Advances in Space Research*, 37:59–66.

Sunshine, J. M., Pieters, C. M., and Pratt, S. F. (1990). Deconvolution of mineral absorption bands - An improved approach. *J. Geophys. Res.*, 95:6955–6966.

Sunshine, J. M., Pieters, C. M., Pratt, S. F., and McNaron-Brown, K. S. (1999). Absorption Band Modeling in Reflectance Spectra: Availability of the Modified Gaussian Model. In *Lunar and Planetary Science Conference*, volume 30 of *Lunar and Planetary Inst. Technical Report*, page 1306.

Vernazza, P., Fulvio, D., Brunetto, R., Emery, J. P., Dukes, C. A., Cipriani, F., Witasse, O., Schaible, M. J., Zanda, B., Strazzulla, G., and Baragiola, R. A. (2013). Paucity of Tagish Lake-like parent bodies in the Asteroid Belt and among Jupiter Trojans. *Icarus*, 225(1):517–525.

Wehner, G. K., Kenknight, C. E., and Rosenberg, D. (1963). Modification of the lunar surface by the solar-wind bombardment. *Planet. Space Sci.*, 11:1257–1261.

Yamada, M., Sasaki, S., Nagahara, H., Fujiwara, A., Hasegawa, S., Yano, H., Hiroi, T., Ohashi, H., and Otake, H. (1999). Simulation of space weathering of planet-forming materials: Nanosecond pulse laser irradiation and proton implantation on olivine and pyroxene samples. *Earth, Planets, and Space*, 51:1265.